AD NUMBER

AD854582

NEW LIMITATION CHANGE

TO

Approved for public release, distribution unlimited

FROM

Distribution authorized to U.S. Gov't. agencies only; Specific Authority; 05 APR 1969. Other requests shall be referred to the Director, Defense Atomic Support Agency, Washington, DC 20305.

AUTHORITY

Per DNA ltr dtd 4 Apr 1972

Gulf General Atomic
incorporated

DASA Report No. 2234
GA-9148

MEASUREMENT OF PROMPT GAMMA-RAYS FROM THERMAL-NEUTRON FISSION OF ^{235}U AND ^{239}Pu, AND FROM SPONTANEOUS FISSION OF ^{252}Cf

---

ANNUAL SUMMARY REPORT
MAY 15, 1967 THROUGH NOVEMBER 30, 1968

Prepared under
Contract DASA 01-67-C-0088
for the
Defense Atomic Support Agency

April 5, 1969

Gulf General Atomic
Incorporated
P.O. Box 608, San Diego, California 92112

DASA Report No. 2234
GA-9148

MEASUREMENT OF PROMPT GAMMA-RAYS FROM THERMAL-NEUTRON FISSION OF ^{235}U AND ^{239}Pu, AND FROM SPONTANEOUS FISSION OF ^{252}Cf

---

ANNUAL SUMMARY REPORT
MAY 15, 1967 THROUGH NOVEMBER 30, 1968

Work done by:

V. V. Verbinski
R. E. Sund
H. Weber

Report written by:

V. V. Verbinski
R. E. Sund

Prepared under
Contract DASA 01-67-C-0088
for the
Defense Atomic Support Agency

Gulf General Atomic Project 6040

April 5, 1969

CONTENTS

ILLUSTRATIONS

1. INTRODUCTION

This annual summary report describes the work performed on the program to measure prompt gamma rays from thermal neutron fission of ^{235}U and ^{239}Pu, and from spontaneous fission of ^{252}Cf from May 15, 1967 through November 30, 1968, under Contract DASA 01-67-C-0088 with the Defense Atomic Support Agency.

One of the primary goals of this research effort was the measurement of the prompt gamma rays from thermal-neutron fission of ^{239}Pu, a measurement which had not been previously reported in the literature. In order to compare these yields directly with other prompt gamma-ray measurements, and to make it possible to determine small differences in the spectral yields for different cases of fission, the prompt-gamma spectral yields for the thermal-neutron fission of ^{235}U and ^{239}Pu and for the spontaneous fission of ^{252}Cf were measured with the same spectrometer system. The differences in the spectra may be due to such parameters as the initial spin of the fissionable nucleus (7/2 for ^{235}U and 1/2 for ^{239}Pu), the excitation energy E^* of the intermediate nucleus, the mode of fission, i. e. , thermal-neutron capture versus spontaneous, and the mass distribution of the fission fragments. On the other hand, the degree of similarity of the spectral yields for these three cases is also of interest since it indicates to what extent the spectral yields may be insensitive to E_n, the incident energy of a neutron that induces fission, and therefore to what degree thermal-neutron fission may produce the same results as fission events produced by incident neutrons of higher energy (14-MeV and fission-spectrum neutrons). The possibility of estimating prompt gamma-ray spectral yields at higher neutron energies from more detailed measurements at thermal-neutron energies is

discussed in the last section of this report.

The parameter E_γ(TOT), the total energy release per fission emitted in the form of prompt gamma rays, has been of interest since the first measurements because E_γ(TOT) was much larger than the early calculations predicted.[1,2] These considerations have led to the conclusion that deexcitation of the fission fragments by neutron emission is inhibited by high angular momentum states of the fragments. Thus, the accurate determination of E_γ(TOT) provides information relating to the initial angular momentum of the fragments.

Earlier measurements of prompt gamma-ray spectral yields have been reported for ^{235}U[3,4] and ^{252}Cf.[5] Many of the shortcomings of these earlier measurements have been overcome in the present measurements by virtue of the following improvements: (1) The fast timing for the fission-fragment and gamma-ray detectors was improved to the point that time-of-flight separation of prompt gamma rays from prompt-neutron-induced counts was achieved; (2) The gamma-ray spectrometer had a nearly localized response over the entire energy range, so that the total spectrum could be obtained with the same detector. The localized responses added much to the accuracy of the data processing in that the unfolding of pulse-height distributions to obtain energy spectra could be done with greater precision. In the limit of a completely localized response (i.e., a gaussian, in the case of a charged particle detector), no unfolding is necessary, and $\varphi(E) = \Psi(E)/\epsilon(E)$, where $\varphi(E)$ is the spectral yield, $\Psi(E)$ the pulse-height distribution, and $\epsilon(E)$ the efficiency; (3) in the design of the present measurements, great care was taken to eliminate the effects of the anistropic angular distribution of prompt gamma rays with respect to the velocity vector of one of the fragments. These design considerations are embodied in the experimental apparatus as described in the following section.

2. EXPERIMENTAL ARRANGEMENT

2.1 CONFIGURATION FOR FISSION FOIL, NEUTRON BEAM AND DETECTORS

Figure 1 is a schematic drawing of the experiment, including detectors and electronics. A thermal beam of neutrons, piped 10 meters from the thermal column of the Gulf General Atomic TRIGA III reactor, provided a flux of 10^6 neutrons/cm^2-sec with a ^{235}U-cadmium ratio of about 350 as determined from the number of ^{235}U fission events without and with a Cd cover. The ^{235}U(n, F) and ^{239}Pu(n, F) events produced in the fissionable material ($\sim$ 10 cm^2 area, 0.2 mg/cm^2 thickness) were detected with a fission-fragment detector of 950 mm^2 area located about 0.25 cm from the fission foil. By keeping this separation small, and by tilting the normal of the foil-detector plane 30° toward the NaI(Tℓ) gamma-ray detector, the effects of the angular distribution between the fission fragment and gamma-ray[6, 7] were minimized. Calculations of these effects were made as a function of possible experimental geometries, and the results showed negligibly small effects for the present setup. For ^{252}Cf(S. F.), the experimental arrangement was the same except that the neutron beam was turned off. The thin ^{252}Cf source (0.01 μg) was obtained from the Oak Ridge National Laboratory (ORNL) Isotopes Division, and high-purity, very clean ^{239}Pu and ^{235}U foils, both > 99.7% enrichment, were provided on a loan basis by F. Kirk Smith and John G. Povelitis of the Los Alamos Scientific Laboratory (LASL).

The fission foil and detector were located in an evacuated chamber with a thin gamma-ray window, and the detector was cooled to -20°C to improve timing and decrease the very large leakage currents produced by radiation damage from fission-fragments and alpha-particle bombardment.

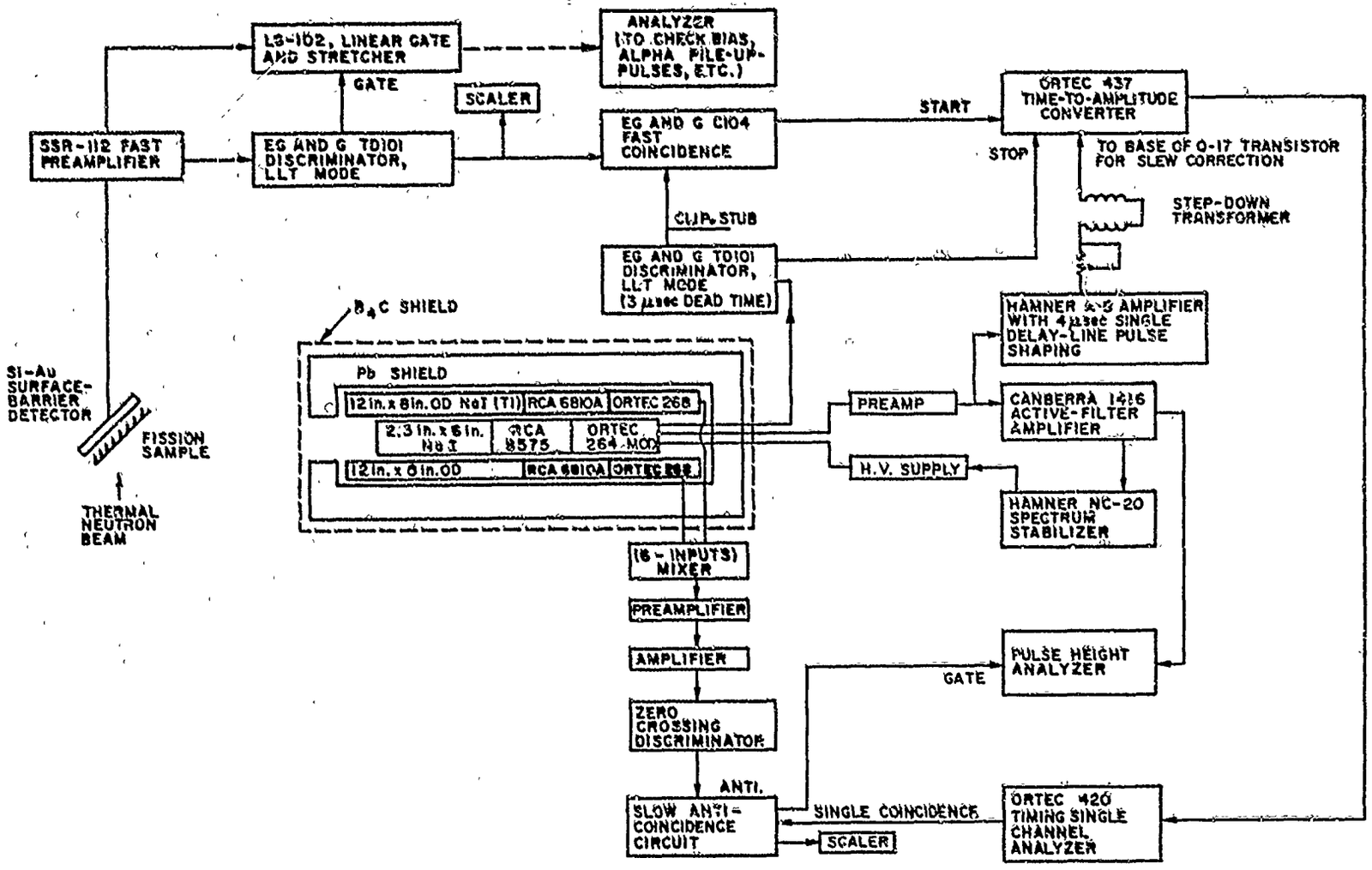

Figure 1. Block diagram of experimental setup and electronics.

The gamma-ray detector consisted of a 5.85-cm-diameter by 15-cm-long NaI($T\ell$) crystal located at the center of a NaI($T\ell$) annulus, 20 cm outside diameter by 30 cm long. A pulse from the center detector was recorded only if there was no simultaneous pulse from the annulus; consequently a nearly localized response was produced as a result of suppressing the Compton-edge and the two annihilation-gamma escape peaks.

2.2 ELECTRONICS

The block diagram in Fig. 1 shows the method used to detect and count fission fragments in the presence of a high alpha-particle count rate for ^{239}Pu and to measure the pulse-height distribution of these gamma rays in coincidence with the fission fragments. By achieving fast timing between the fission fragment and gamma ray, it was possible to achieve good time separation between the gamma-ray pulses and the pulses due to effects of the fission neutrons which had to travel 70 cm to reach the gamma-ray detector. The flight times are ~ 50 nsec and 15 nsec for 1 and 10 MeV neutrons, respectively.

Pulses from the fission-fragment detector and fast preamplifier were sent to a linear gate and stretcher, and to a fast, double-level, leading-edge discriminator operated in the lower level timing mode. The discriminator level was determined by observing the output of the linear gate and stretcher on a pulse-height analyzer. Output pulses from the discrimination circuit were used to gate on the linear gate and stretcher for 35 nsec. This reduced alpha-particle-pileup effects for pulses stored in the analyzer to a negligibly small value, and made it possible to observe a conservative estimate of these effects. The ratio of the biases for the double-level discriminator was 3 to 1; both biases were above the alpha-particle levels.

The output of the fission-fragment discriminator was delayed and sent to a fast coincidence circuit which was also fed by the fast-discriminator

output of the central NaI(Tℓ) gamma-ray detector. The timing of the fast coincidence output was determined by the timing of the fission-fragment pulse. This output was used as a START signal for the time-to-amplitude converter (TAC). The STOP signal for the TAC was obtained from the same fast gamma-ray discriminator referred to above, a double-level discriminator set at 20 keV and 50 keV gamma-ray energy. This discriminator was fed with the fast anode pulses from the central NaI photomultiplier tube. The timing curve shown in Fig. 2 was obtained with the use of this discriminator operating in the lower level timing mode, and with a slew correction signal obtained from the central gamma-ray detector and added to a summing junction in the TAC, as shown in Fig. 1. The output of the TAC was interrogated with a single channel analyzer with upper window set in the valley between the prompt gamma-ray peak and the broad peak due to prompt-neutron effects (at about 10 nsec after the gamma-ray peak) and with the lower window set about 12 nsec to the left of the peak (see Fig. 2). Without slew correction the valley just to the right of the gamma-ray peak for pulses below 0.2 MeV was displaced $\sim$ 5 nsec with reference to the corresponding valley for pulses > 2.0 MeV. Thus, the slew correction was important in achieving good gamma-neutron separation.

Continuing with the block diagram, the proper pulses from the TAC were placed in anticoincidence with pulses from the large NaI anticoincidence annulus, which had a discriminator bias of 35 keV. The resultant pulse was used to gate on the analyzer. The spectrum stabilizer, shown in Fig. 1, was used to eliminate drifts in gain encountered with long counting times and with some changes in count rate. The ORTEC model 264 photomultiplier tube base showed some nonlinearity and count rate drifts as used with the RCA 8575 photomultiplier tube. These were reduced appreciably by attaching additional stabilizing capacitors from ground to an unstabilized dynode and the focus grid, and by increasing the current through the voltage-divider string by a factor of three (by changing

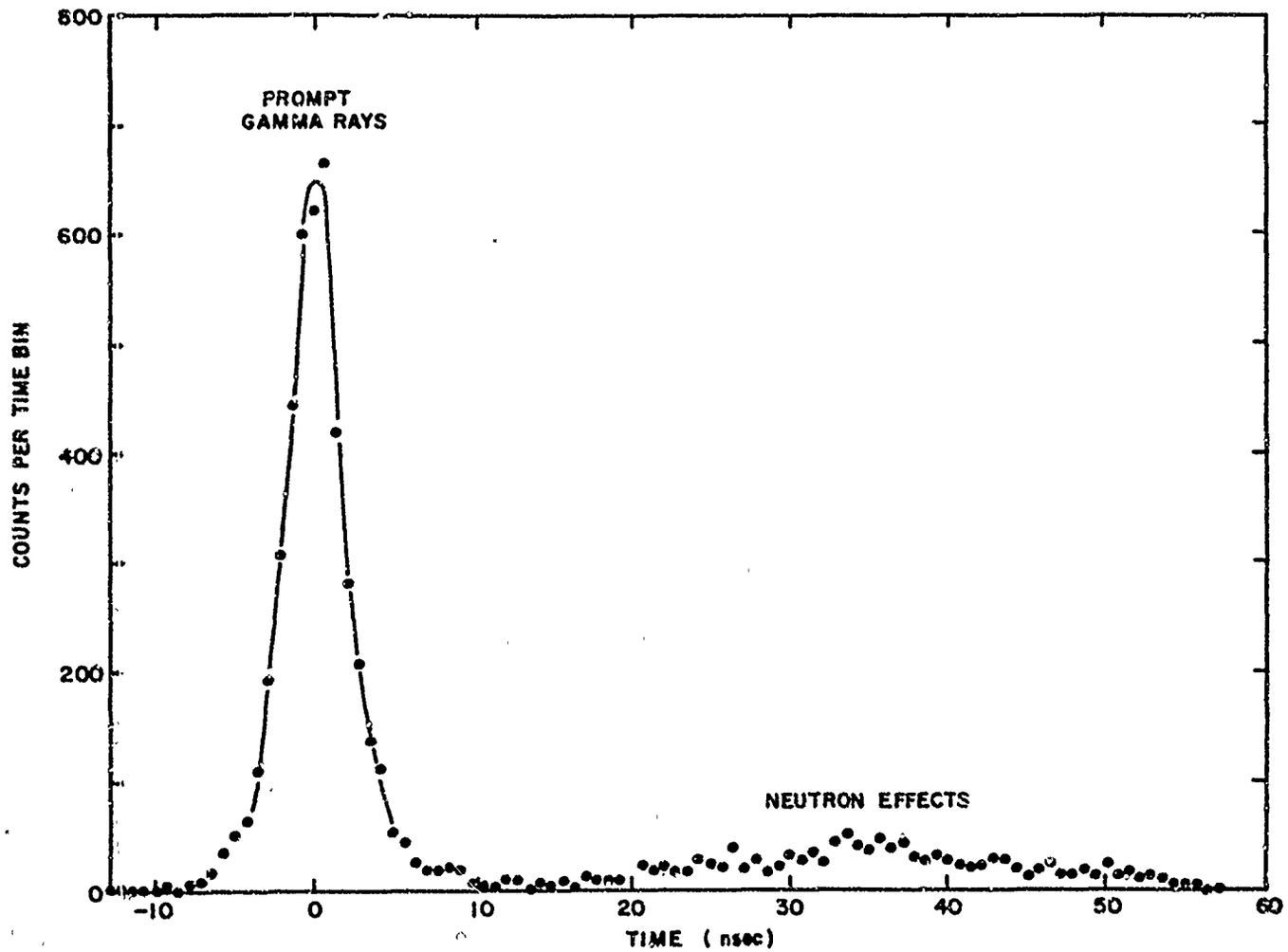

Figure 2. Intensity of gamma ray events observed with the present spectrometer as a function of time after the detection of ^{252}Cf fission fragments. The zero time given in the figure was arbitrarily adjusted to the center of the strong peak.

resistors). The fast output from the 8575 tube caused multiple pulsing of the fast discriminator due to the long decay time of light from NaI(Tℓ). These were eliminated by utilizing a large deadtime for the discriminator. With the experimental counting rates for the center detector and annulus, the maximum deadtime was 2%; the data were corrected for deadtime effects.

2.3 BACKGROUND PROBLEMS

The background counts were caused by chance coincidences between fission-fragment pulses and gamma-ray pulses. These were measured by increasing the delay for the fast gamma-ray pulse between the double level discriminator and fast coincidence circuit. In this way, we observed the chance events occurring just before the fission event occurred. The total background count rate was 1/2000 of the real rate for the ^{252}Cf(S. F.) measurements and about 1/200 of the real rate for ^{235}U(n, F) and ^{239}Pu(n, F). The slow neutron beam, which was present only for the latter two cases, produced a high gamma-ray count rate from neutron scattering from, and captures in, the ^{235}U, the ^{239}Pu, and the surrounding material, and from neutron capture in the NaI(Tℓ). Tight beam collimation reduced the capture gamma rays in the material near the ^{235}U and ^{239}Pu, and the lead gamma-ray shielding and boron carbide slow-neutron shielding surrounding the NaI detectors reduced scattered neutron effects to a reasonable level.

As discussed above, backgrounds due to fast neutrons arriving at the detector before closing the time-gate were reduced to a negligibly small level (~ 1%) by setting the right edge of the time gate to the right of the gamma-ray peak (see Fig. 2). A measurement was made with the time-gate adjusted to accept pulses falling from 10 to 50 nsec after the gamma-ray peak for ^{235}U(n, F). These produced approximately 15% of the intensity observed for prompt gamma rays from fission, and gave a rough estimate of the error that can arise from measuring prompt gamma

rays with this detector system without any elimination of the prompt-neutron effects. The pulse-height spectrum for the delayed pulse was somewhat similar to that for prompt gamma rays from fission.

3. DETECTOR RESPONSES AND CALIBRATIONS

3.1 FISSION-FRAGMENT DETECTOR

A pulse-height distribution from the fission-fragment detector is shown in Fig. 3. A representative bias level is also shown in the figure. The pulse-height distribution deteriorated with radiation damage to the detector, with the result that the depth of the valley between the two peaks slowly decreased with exposure to fission fragments and alpha-particles. Also, the number of deteriorated pulses near the bias level increased with radiation damage; however, this number was always small because of replacement of detectors after moderate radiation damage. The effective life of the detectors was prolonged appreciably by cooling them to -20°C, where the large radiation-damage-induced leakage currents were reduced by about an order of magnitude. Cooling also improves the fast timing by reducing the noise and by improving the charge-carrier mobility.

3.2 GAMMA-RAY DETECTOR RESPONSE CURVES

The LSMUN code described below requires as an input the shapes of the detector response to 200 monoenergetic gamma-ray lines uniformly spaced in energy. These responses constitute the response matrix G(I, J) for 200 values of gamma-ray energy E(J). The matrix is computed by a set of response equations whose parameters are obtained as a function of E(J) from fitting the response equations to measured gamma-ray pulse-height distributions, as shown in Fig. 4. The parameters of the response equation that vary with energy include the width of the gaussian-like photopeak, the peak area (discussed below in Section 3.3, "Efficiency Measurements"), the relative areas of the single and double escape peaks for

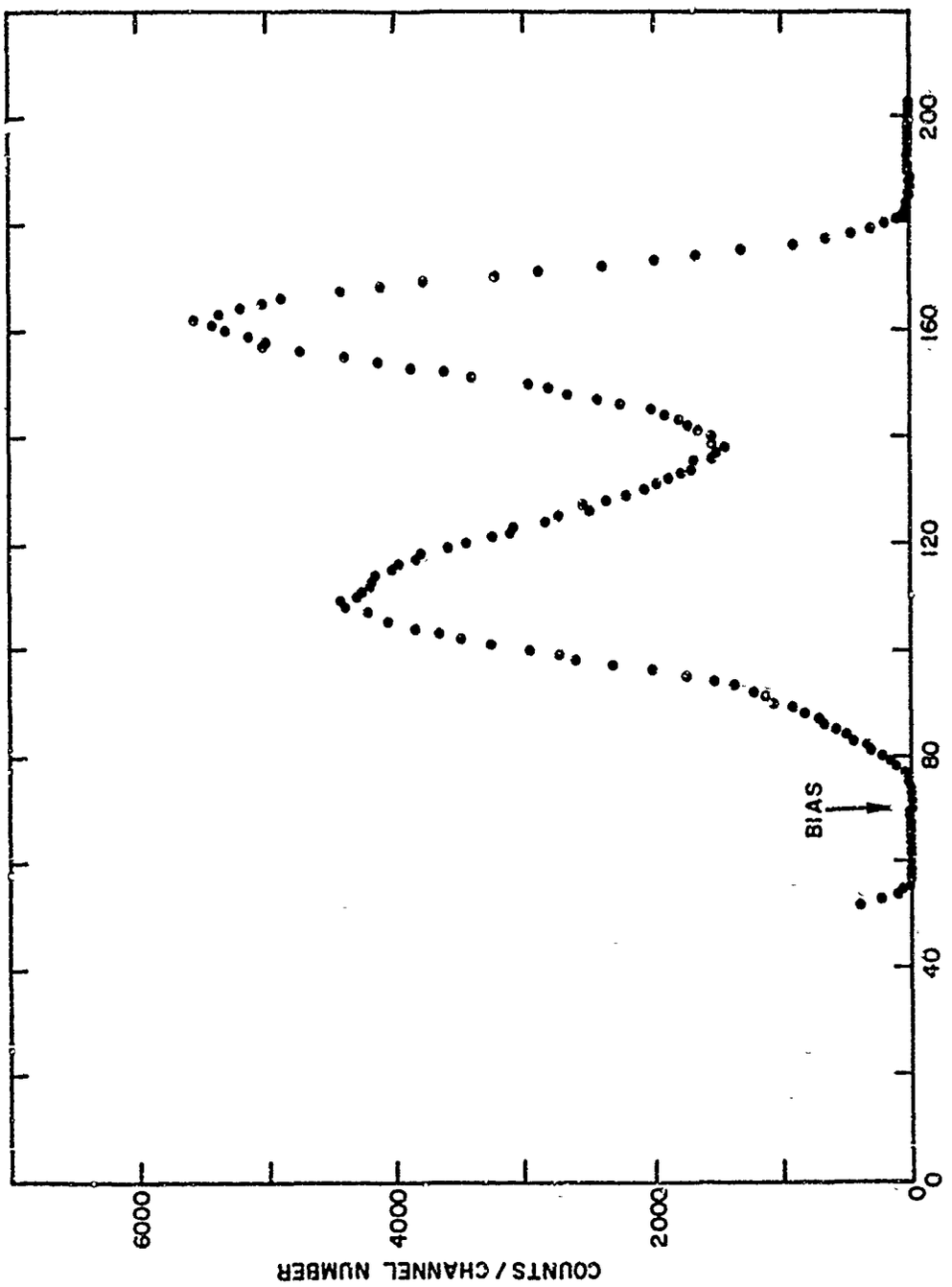

Figure 3. Energy spectrum of ^{235}U fission fragments, as observed in the present experimental arrangement. The discriminator bias used in taking the prompt gamma-ray data is indicated.

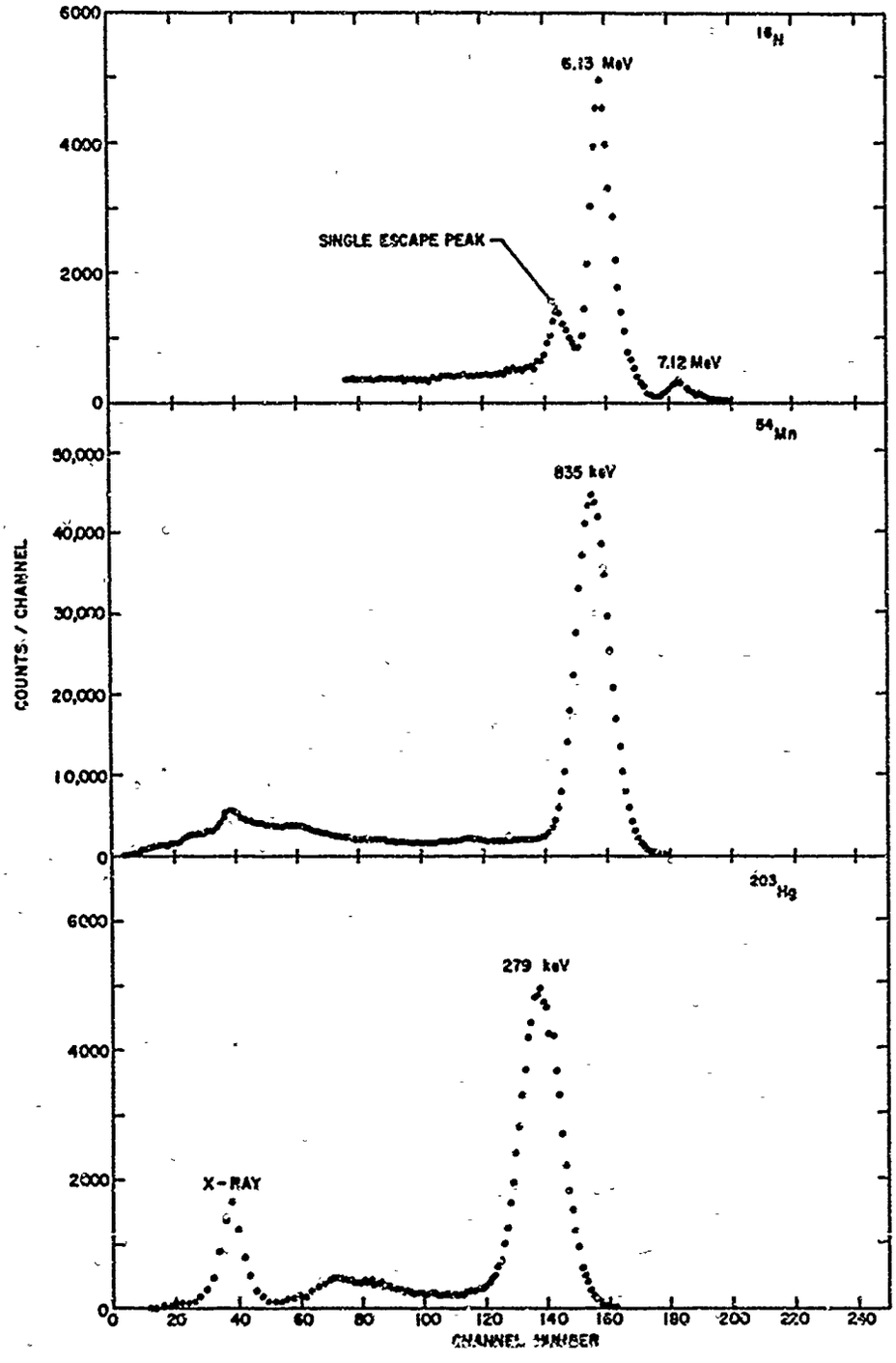

Figure 4. NaI pulse height distributions for the gamma rays following the decay of ^{16}N, ^{54}Mn, and ^{203}Hg.

$E(J) > 1.02$ MeV, the height and "edge shape" of the Compton scattering plateau, and the width and height of the source-backscatter peak. These parameters, as well as the form of the response equations, were determined by us for our detector configuration.

Measurements of responses were made by placing radioactive gamma-ray sources in the precise position of the fission-foil source, whenever possible, and surrounding them with the same materials such as fission detector, vacuum chamber, and windows. In this way the attenuations and source-backscatter peak were correctly reproduced. The gamma-ray sources and corresponding lines were: ^{57}Co at 0.122 MeV, ^{203}Hg at 0.279 MeV, ^{22}Na at 0.511 and 1.275 MeV, ^{137}Cs at 0.662 MeV, ^{54}Mn at 0.835 MeV, ^{88}Y at 0.90 and 1.84 MeV, ^{24}Na at 1.37 and 2.75 MeV, a PuBe source at 4.44 MeV [from the reaction ^{9}Be(α, n) ^{12}C$^{*} \rightarrow 4.44$ MeV, with the use of careful paraffin-lead shielding], and ^{16}N(7.1-sec half-life) at 6.13 and 7.12 MeV. The latter source was obtained from ^{16}O(n, p) ^{16}N reactions in the cooling water passing through the TRIGA III reactor. The cooling water was pumped from the top of the reactor to a small reservoir located 70 cm from the detector. The spectra for ^{203}H, ^{54}Mn, and ^{16}N are shown in Fig. 4.

Some of the above sources had two gamma rays. The shapes of the backscatter peak and the lower part of the Compton distribution for the 1.275-MeV gamma ray from ^{22}Na were determined from the spectrum of the 1.33- and 1.17-MeV gamma rays from ^{60}Co. In this way, the response function for the 1.275-MeV gamma ray from ^{22}Na could be separated from that of the 0.511-MeV annihilation radiation from the same source. The contribution of the 1.37-MeV line to the 2.75-MeV line of ^{24}Na was subtracted by scaling up the 1.275-MeV line of ^{22}Na to 1.37 MeV, and the 0.90-MeV contribution from the 1.84-MeV line of ^{88}Y was determined by using the 0.84-MeV line of ^{54}Mn. With these techniques, the entire pulse-height distributions could be obtained for energies up to 2.75 MeV. Since the data for the higher-energy gamma

rays were poor at the lower parts of the response functions as a result of background problems, we extrapolated this information from parameters that described the data for gamma rays at 2.75 MeV and below. Because the steep NaI pulse-height distributions obtained in the prompt gamma-ray measurements presented here, the accuracy of the low-energy portion of the response functions for large E(J) is not important.

3.3 EFFICIENCY MEASUREMENTS

For energies up to 1.84 MeV the photopeak efficiency $\epsilon(E)$, determined by the number of counts within twice the full width at half maximum, was measured with sources calibrated at several places, including the National Bureau of Standards (NBS), LASL, New England Nuclear Corporation (NENC), and CIA (France). The sources were placed at the normal position of the fission foil, so the experimental geometry was included in the determination. In Fig. 5, $\epsilon(E)$ is shown for various energies from 0.122 to 7.12 MeV, along with estimated errors. The most accurate calibration points were those for the 0.511 and 1.275 MeV lines of ^{22}Na, as obtained from a source calibrated both at NBS and LASL, and from another calibrated ^{22}Na source from NENC. A source uncertainty of ±2.8% was estimated for these two calibration points. The calibration points at 0.122, 0.279, 0.511, 0.662, 0.90, 1.275 and 1.84 MeV were plotted and a smooth line could be drawn through the points obtained with sources from suppliers or calibration laboratories listed above. Sources from other suppliers that gave some bad points were not used.

An efficiency calibration at 2.75 MeV was performed with a ^{24}Na source, utilizing the fact that the intensities of the 1.38- and 2.75-MeV gamma rays are equal. The ^{24}Na was made from chemically pure NaF exposed to neutrons from a reactor. At 4.44, 6.13, and 7.12 MeV, calibrations were carried out by cross calibrating against a 2-in. by 2-in.-diameter NaI(Tℓ) crystal which in turn had been calibrated by Jarczyk, et al.[8] We checked Jarczyk's calibration at 2.75 MeV against our

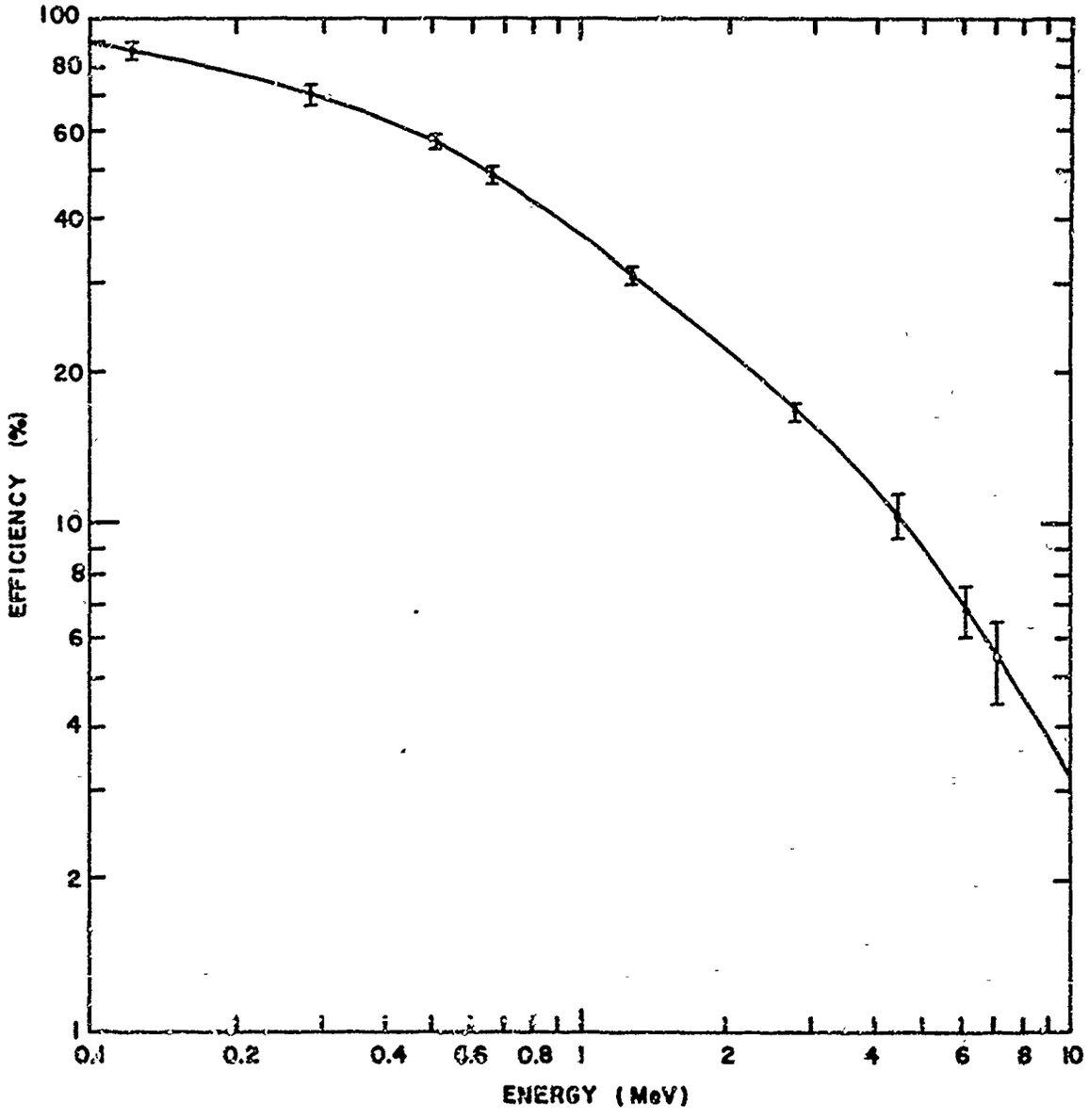

Figure 5. Absolute photopeak efficiency of the NaI spectrometer for detecting gamma ray events. The effect of the present experimental geometry is included in these data.

independent method, and obtained agreement well within the 3% error on this point quoted by Jarczyk, et al.[8] The error bars shown in Fig. 4 include the errors quoted by Jarczyk and the statistical and estimated systematic errors for our cross-calibration procedure.

4. DATA HANDLING TECHNIQUES

4.1 PULSE-HEIGHT DISTRIBUTIONS

The pulse-height distribution for the total counts and background counts were processed to obtain the net counts and the standard deviations. The data were then processed with an unfolding code that converted the NaI pulse-height distributions to absolute spectral flux. To improve the accuracy of the low-energy data, the data were taken for two gain settings, and a double-unfold method was devised to extend the range of the unfolding code. The errors on the unfolded data were then derived.

4.2 UNFOLDING CODE

The LSMUN code[9] calculates a response matrix G(I, J) with the energy mesh that corresponds to the pulse-height distribution of the raw data. After the shapes are calculated, the photopeak efficiencies are used to determine the absolute spectrum for the experimental geometry. As mentioned above, in Section 3.2, the response matrix is calculated with a response equation whose parameters are determined by fitting the response curves to measured pulse-height distributions. The response equations, parameters, and the efficiency table had to be determined for our detector configuration. The LSMUN code utilizes this information to calculate the energy spectrum $\phi(E_j)$ from the raw pulse-height distribution y_i as indicated below.

The pulse-height distribution $\vec{Y}$ is related to the spectrum $\vec{\phi}$ and the instrument response matrix $\bar{\bar{G}}$ by

$$\vec{Y} = \bar{\bar{G}}\,\vec{\phi} \qquad (1)$$

However, the solution

$$\phi = \bar{\bar{G}}^{-1} \vec{Y} \tag{2}$$

oscillates violently for most cases, and smoothing of some sort must be done.

The LSMUN code embodies the method of B. C. Cook[10] to accomplish this. Utilizing the calculus of variations, Eq. 1 takes the form

$$(\bar{\bar{G}} + \lambda (\bar{\bar{G}})^{-1} \cdot (\bar{\bar{W}})^{-1} \cdot \bar{\bar{S}}) \vec{\phi} = \vec{Y} \tag{3}$$

where $(\bar{\bar{G}})^{-1}$ is the inverse of the transposed $\bar{\bar{G}}$ matrix, $\bar{\bar{S}}$ is a smoothing matrix determined by a structure function $S(\phi)$ which is arbitrary within limits. Some typical expressions for $S(\phi)$ are $S_1(\phi)$, which is a function of the first derivative or slope of the solution ϕ, and S_2, which is a function of the second derivative or curvature of ϕ (i.e., $S_1 = S_1(\phi_{j+1} - \phi_j)$, $S_2 = S_2(\phi_{j+1} - 2\phi_j + \phi_{j+1})$). $\bar{\bar{W}}$ is a diagonal matrix with elements $W_{ii} = (1/\Delta y_i)^2$ and thus contains weighting factors which become small in the vicinity of a gamma-ray peak in ϕ_j, and λ is a Lagrangian multiplier.

An initial value of λ is used as an input to LSMUN, and the code then obtains a solution to Eq. 3 for $\vec{\phi}$. This solution is then multiplied by $\bar{\bar{G}}$, as in Eq. 1, and the energy spectrum ϕ is thus refolded to get the precise value of $\vec{Y}$ that corresponds to $\vec{\phi}$. A χ^2 test is performed utilizing the differences $(\tilde{y}_i - y_i)$ where $\tilde{y}_i$ correspond to the refold of the first solution $\vec{\phi}$ and y_i to the raw data in channel i. The value of λ is varied in an iterative manner to obtain a value of $\chi^2 \simeq N$, where N is the number of channels, which is limited to 200 by the computer memory (matrix size $\sim$ 40,000 words).

The LSMUN code was tested for self-consistency by determining the accuracy with which it can unfold single- and multiple-line gamma-ray sources of known source strength. The code was found to be self-consistent at all energies within a few percent; the error indicated in the self-consistency test happened to be always significantly less than the error

bars on the efficiencies. At low channels, where the full width at half maximum of the photopeak was less than two channels wide, the LSMUN code produced normalization factor errors. These were computed, and the corresponding correction factors were applied to the code.

4.3 DOUBLE UNFOLDING

The code normally covered the range from 0.3 to 10 MeV, whereas the lower energy limit of the NaI pulse-height distribution was 0.07 MeV, as determined by the discrimination setting for the center detector. To overcome the resolution limit of the unfolding code at the low-energy end and to extend the range to lower energies, we made use of an additional high-gain (low energy) run and double-unfolded the data. This low-energy unfolding was accomplished by first unfolding the high-energy data to obtain $\phi(0.3 \rightarrow 10$ MeV), and then folding back in $\phi(1 \rightarrow 10$ MeV) by having Eq. 1 operate on the spectrum above 1 MeV. This folded-in pulse-height distribution was then subtracted from the high-gain (low energy) raw data, yielding the NaI pulse-height distribution that would have resulted if all gamma rays above 1 MeV had been absent. The net high-gain pulse-height distribution (below 1 MeV), along with the correct standard deviations resulting from the Compton-tail subtractions for gamma rays above 1 MeV, were then used as input to LSMUN, which provided $\phi(E)$ with good energy resolution and reasonable accuracy down to 140 keV, below which the energy spectrum drops rapidly.

To eliminate any oscillations in the high-gain unfolded results, the unfolding was done with a reduced photopeak width as compared to the actual experimental width; in this procedure, the proper photopeak efficiency and the proper ratio for the Compton height to photopeak area were maintained. This resulted in accurate values for the energy per fission and the number of gamma rays per fission, although the peaks in the unfolded spectrum should be somewhat less pronounced than in the actual gamma-ray spectrum striking the detector.

4.4 EXPERIMENTAL ERRORS

The most important sources of experimental errors are counting statistics, detector-efficiency calibration, generation of the response-matrix, and unfolding the data.

The nearly singular response functions of our detector and the rapidly falling spectrum facilitated a reasonably straightforward calculation of the statistical error for the unfolded spectrum, $\phi(E_k)$. The fractional error on $\phi(E_k)$ may be obtained by adding in quadrature the fractional errors on the two components of the raw data y_k, i.e., the "photopeak counts" y'_k due to photons of energy E_k and the Compton-tail (plus escape) counts y''_k in channel k that are due to photons of energy greater than E_k. y''_k is obtained by refolding that part of the spectrum $\phi(E_k)$ that lies above E_k. Since $y'_k = y_k - y''_k$, the photopeak contribution to the error is simply $\sigma_p = \sqrt{y'_k}$. The error σ_c on y''_k, the Compton-tail contribution, is derived from the fractional error on the "photopeak counts" above E_k to which the Compton-tail counts belong. This is done with the use of the response matrix G(I, J) and, in addition, multiple refolding is utilized. Since σ_c is typically much smaller than σ_p, particularly at high energies, the overall error on $\phi(E_k)$ could be obtained with good accuracy. These calculations of σ_c were carried out with some conservative simplifying assumptions. The ratio y'_k/y_k of "photopeak counts" to total counts in a given channel k was about 0.8 above 0.7 MeV and 0.7 at about 0.25 MeV. This ratio decreases rapidly below 140 keV, where the input pulse-height distribution is falling rapidly. This means that at energies below 100 keV, the counts are mostly due to Compton-scattering events from higher energy gamma rays.

At about 0.10 MeV, the unfolding error due to small inaccuracies in the height of the Compton-tail is much larger than the statistical error. This led us to show no data below 0.14 MeV. To estimate errors such as these that are associated with response-function inaccuracies, a typical

low-gain spectrum was unfolded with the Compton-tail portion increased by 20%. This is considerably more than our fitting-error for the response functions. The corresponding error on the spectral shape was less than the combined uncertainties due to counting statistics and detector-efficiency measurements (see Sec. 3.3). In addition, the total gamma-ray energy per fission above 0.14 MeV, $E_\gamma(TOT)$, changed by only 2%.

Coding errors were found at low channel numbers due to finite channel widths, as mentioned at the end of Sec. 4.3, but the appropriate corrections reduced this source of error to a relatively insignificant amount. The accuracy of the unfolding code was always checked by carrying out the refold of $\phi(E)$ according to Eq. 1. This refold was accurate because it utilized the direct response matrix G(I, J), without the conditioning terms used in the unfolding matrix of Eq. 3. Some small, local corrections had to be applied to $\phi(E)$, and the validity of these "perturbation corrections" checked by refolding the corrected $\phi(E)$. The agreement was then found to be very good. Thus, it is reasonably certain that the dominant error on the spectrum arises from detector-efficiency calibration, except at high energies, where $\phi(E)$ is small and the statistical error large. It then follows that the dominant error on the integrated quantities, such as $E_\gamma(TOT)$, results from the detector efficiency calibration. The efficiency effects on $E_\gamma(TOT)$ are about 3%. A conservative overall error of 5% is suggested, or about ± 0.3 MeV on $E_\gamma(TOT)$.

5. RESULTS

In Fig. 6 is shown the NaI pulse-height distribution for prompt fission gamma-rays from ^{235}U, and below it the unfolded energy spectrum of gamma rays per fission fragment. At higher energies the data have been grouped, as indicated by the spacing of the points in the figure. Below 0.7 MeV, the high-gain NaI data and the results of the double unfolding are shown. We compared the high-gain raw data with the low-gain data in the overlap region of 0.6 to 0.8 MeV, both normalized to the same number of fission events and the energy width of the analyzer channel. The agreement was good for the raw data and also for the unfolded data, which were similarly checked. The same structure that appears in the pulse-height distribution, y_i, below 1 MeV can also be seen in the unfolded energy spectrum shown in Fig. 6. Most of the difference in the shape of the two curves is due to the shape of the efficiency curve $\epsilon(E)$. In fact, with the very localized responses that result from the use of the anti-coincidence annulus, at all points on the pulse-height distribution where the slope is negative and steep, $\phi(E)$ is only slightly less than $y_i/\epsilon(E)$, where i is proportional to E. At high energies the unfolded data appears smoother than the pulse-height distribution because of the smoothing routine in the unfolding code, as explained in Sec. 4.2. The error bars shown in the figure on the raw data, as well as the unfolded data, represent only the statistical uncertainties. In addition, there are systematic errors which are mostly due to the efficiency calibration of the gamma-ray detector, as discussed above (see Fig. 5).

Due to Doppler effects arising from the motion of one of the fission fragments, about half of the structure in Fig. 6 would be more pronounced if it had been measured for all heavy fragments striking the detector

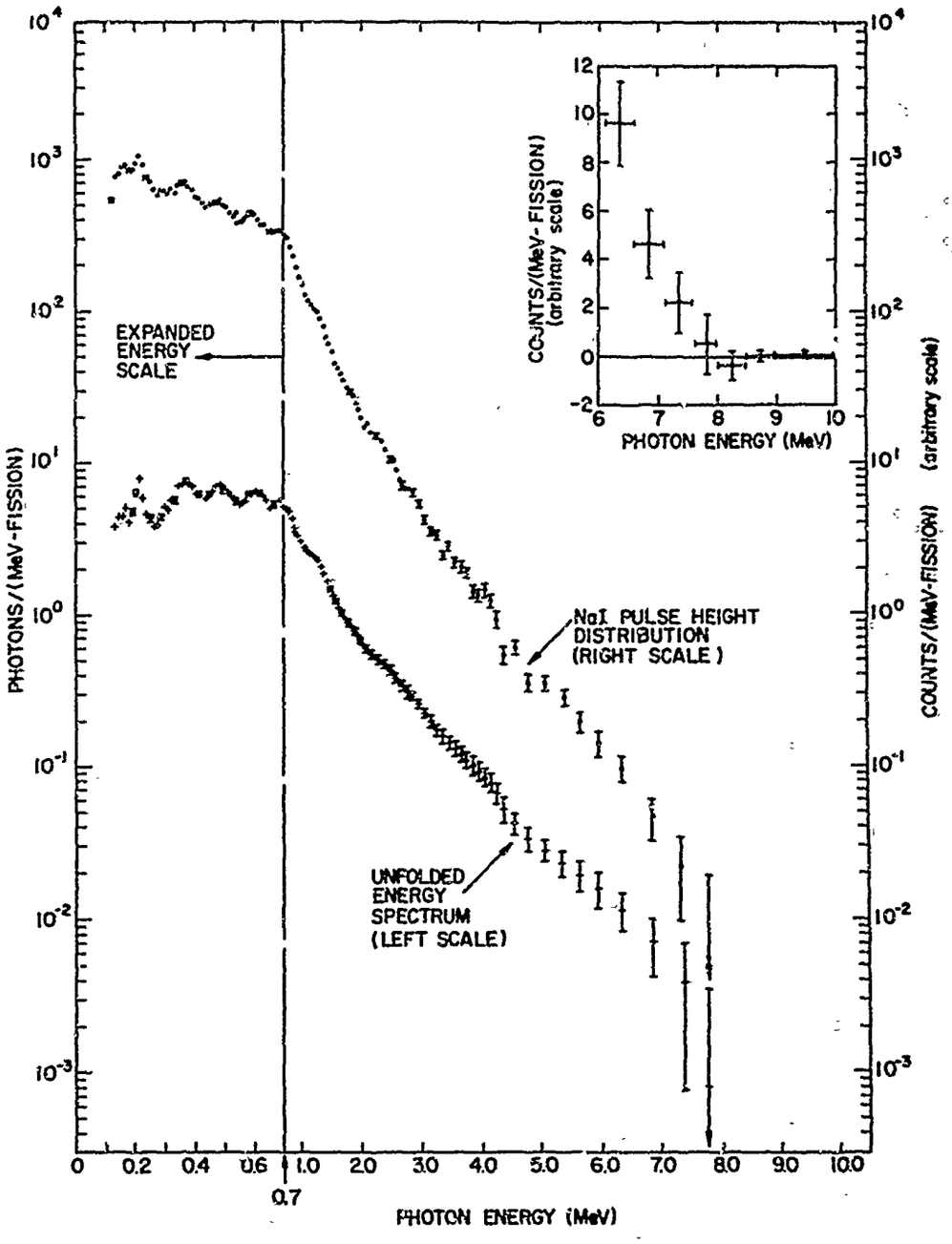

Figure 6. NaI pulse height distribution from the thermal-neutron fission of ^{235}U. The insert shows the data at high energies on a linear scale. Also shown is the unfolded spectrum. The difference between the shapes of the two curves is primarily due to the change in efficiency with energy. The error bars are too small to show in the 0.7 to 1.5 MeV region.

(lower peak in Fig. 3) and the other half of the peaks would be sharper if the gamma-ray spectrometer had been gated on only for light-fragment counts. According to the measurements of Johansson, et al., [11] most of the prompt gamma rays are emitted between 10^{-12} and 10^{-9} sec. The stopping time of the fragments is about 10^{-12} sec in the fission-foil backing, and the travel time to the detector is $\sim 10^{-9}$ sec. Therefore, the Doppler shift affects only the prompt gamma-rays emitted from the fragment that strikes the detector.

Figures 7 and 8 show similar results for ^{239}Pu and ^{252}Cf. A comparison of our results for ^{235}U, ^{239}Pu and ^{252}Cf is given in Fig. 9.

In Fig. 10 is shown the ^{235}U prompt gamma-ray spectrum compared with the data from ORNL, Reference 12, where recent improved efforts at reprocessing the old (circa 1958) data[3] have been reported. The agreement is good at high energies, but gets worse with decreasing energy. The higher values obtained at ORNL are consistent with the possibility of additional counts from fission-neutron effects on NaI; however, we cannot rule out the possibility that a significant portion of the disagreement arises from other sources of uncertainty, such as the detector efficiency, the response shapes and unfolding code problems that are to some degree common to both sets of measurements.

In Table 1 the energy emitted per fission event in the form of prompt gamma radiation and the number of gamma rays per fission are given for a number of energy intervals above 0.14 MeV; the errors are given in the caption. The difference between our data and the ORNL results for the integrated gamma-ray yield above 0.3 MeV is just slightly outside the combined error bars on the two sets of data. Our results for $E_\gamma > 0.3$ MeV are 6.33 ± 0.30 MeV/fission, including estimated systematic errors, while the ORNL results[12] are 7.14 ± 0.42 MeV/fission, if one linearly adds the 0.1 MeV statistical to the estimated 6% systematic error. Our ^{235}U value of $E_\gamma(\mathrm{TOT}) = 6.51 \pm 0.30$ MeV/fission for $E_\gamma >$ 0.14 MeV is well below the value of 9.5 ± 0.23 MeV/fission above

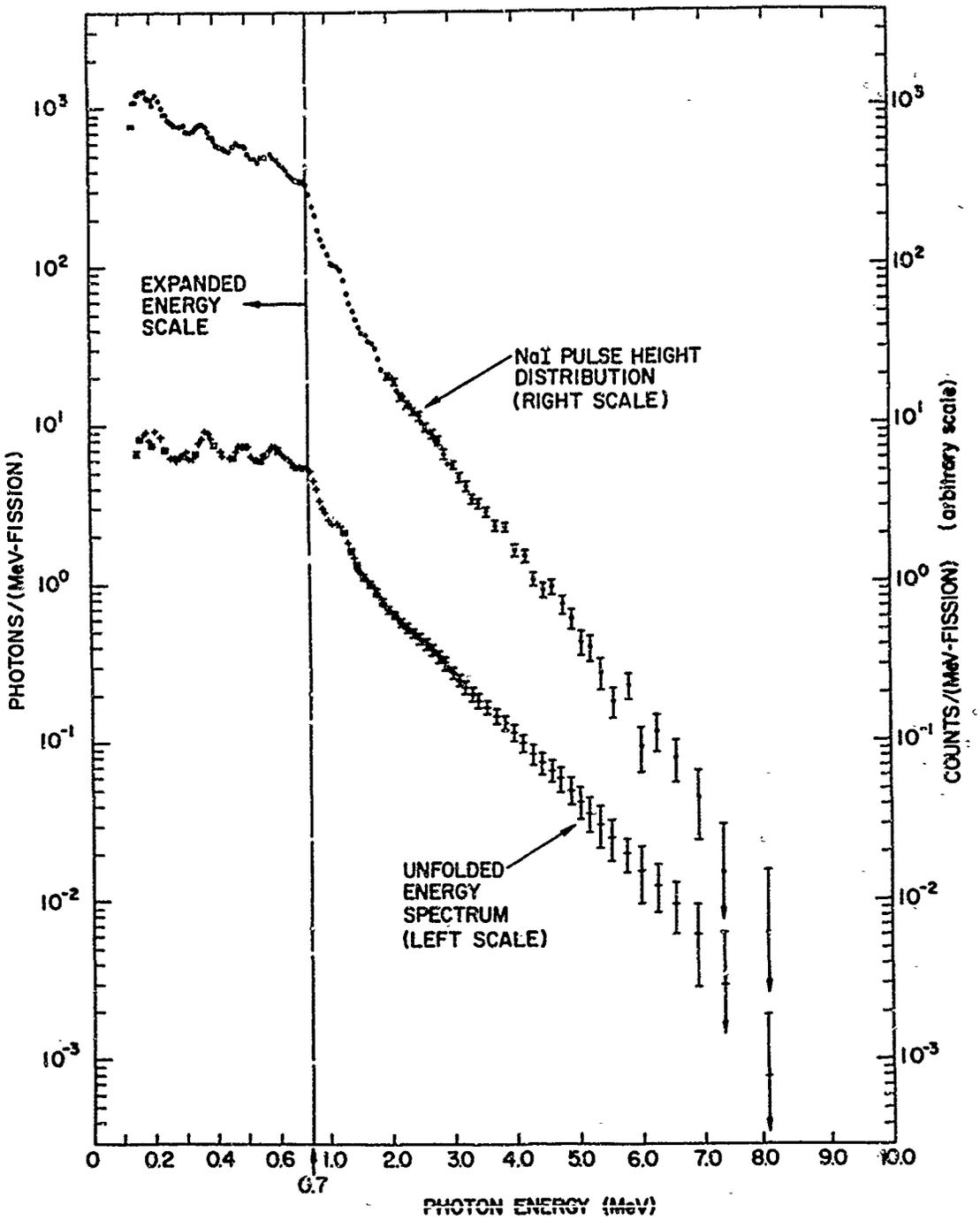

Figure 7. NaI pulse height distribution for prompt gamma rays from the thermal-neutron fission of ^{239}Pu. Also shown is the unfolded spectrum. The error bars are too small to show in the 0.7 to 1.5 MeV region.

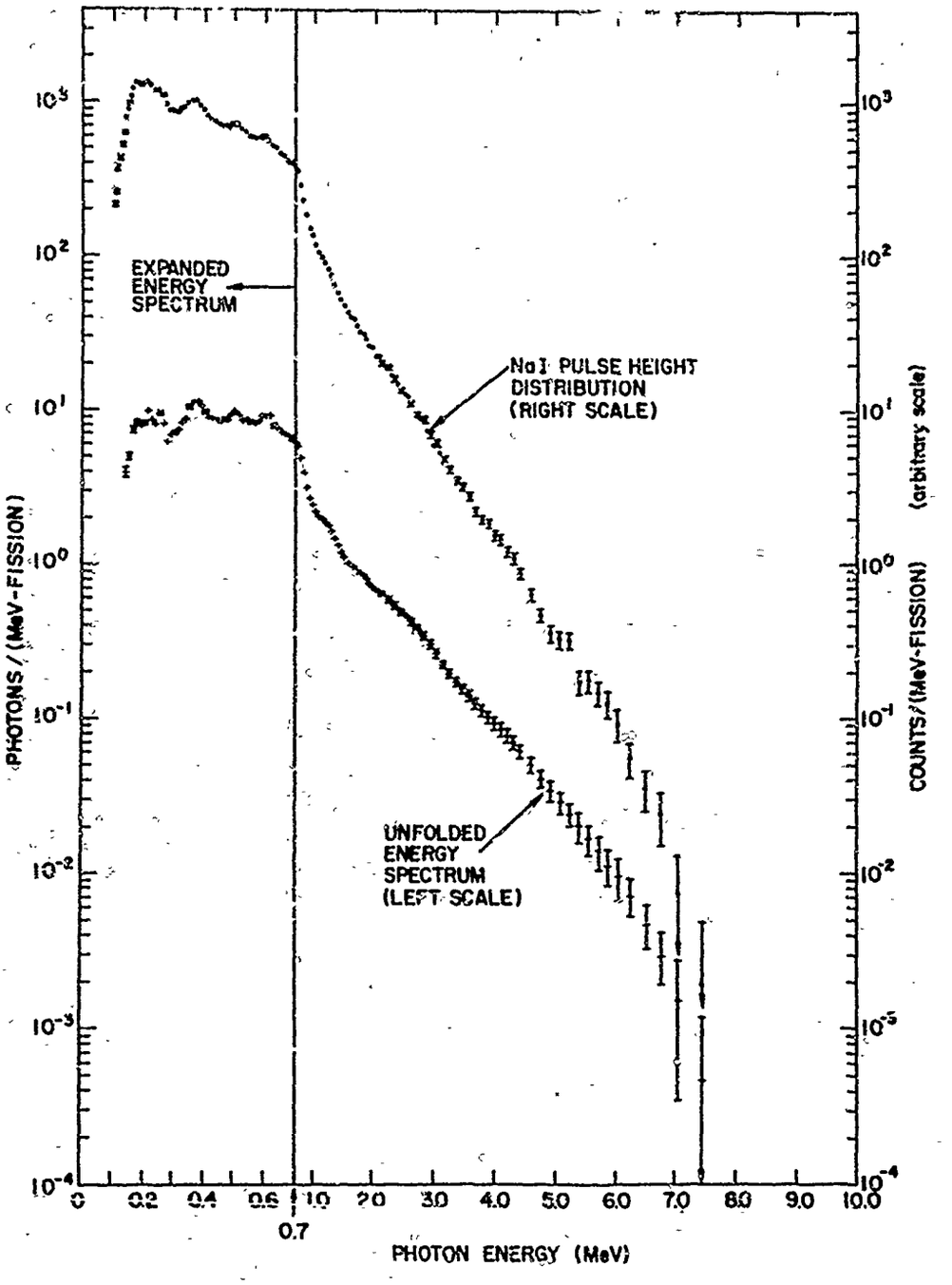

Figure 8. NaI pulse height distribution for prompt gamma rays from the spontaneous fission of ^{252}Cf. Also shown is the unfolded spectrum. The error bars are too small to show in the 0.7 to 2 MeV region.

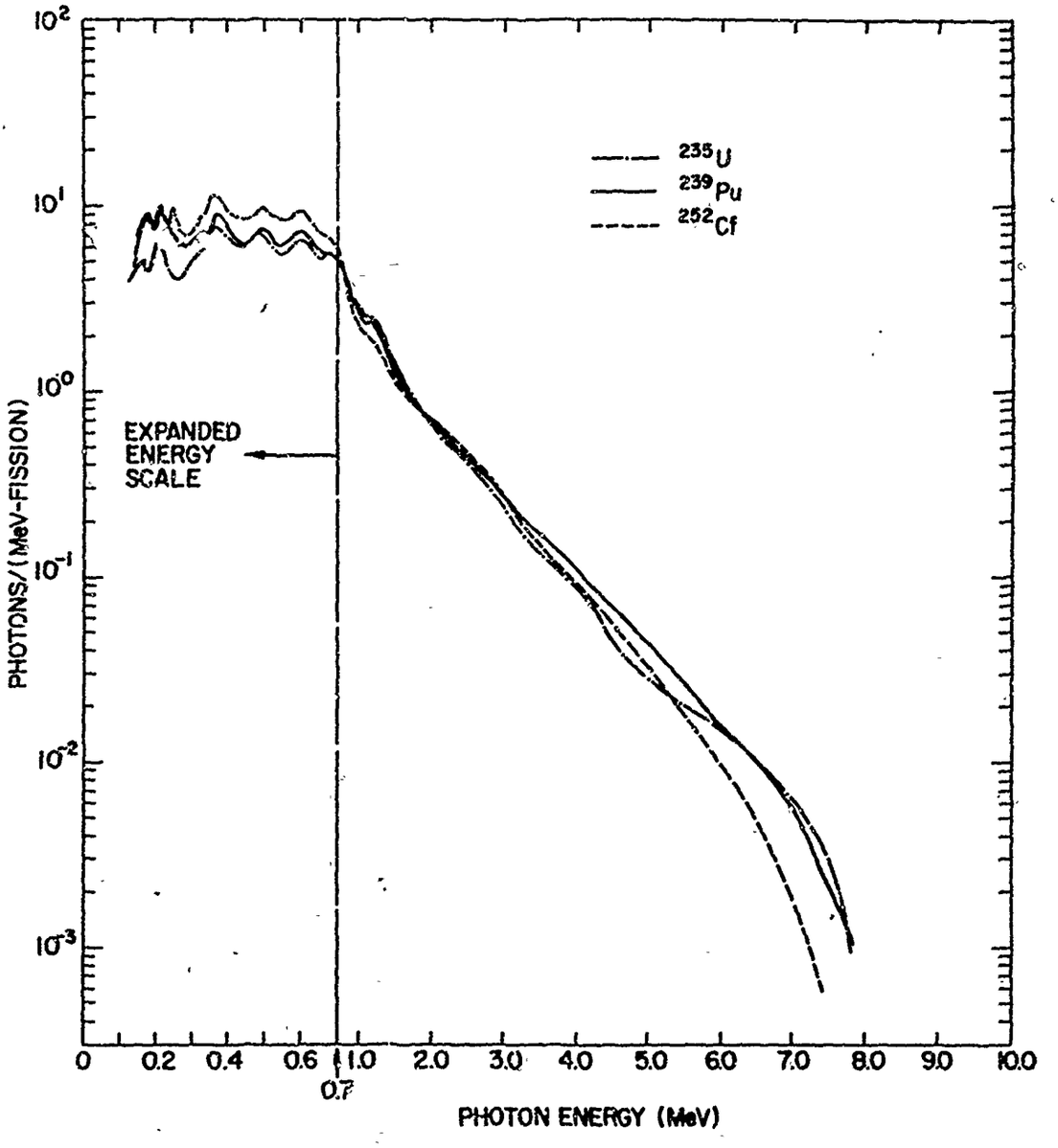

Figure 9. Unfolded prompt gamma-ray energy spectra for the thermal-neutron fission of ^{235}U and ^{239}Pu and for the spontaneous fission of ^{252}Cf. The error bars on the unfolded data are indicated in Figs. 6 - 8.

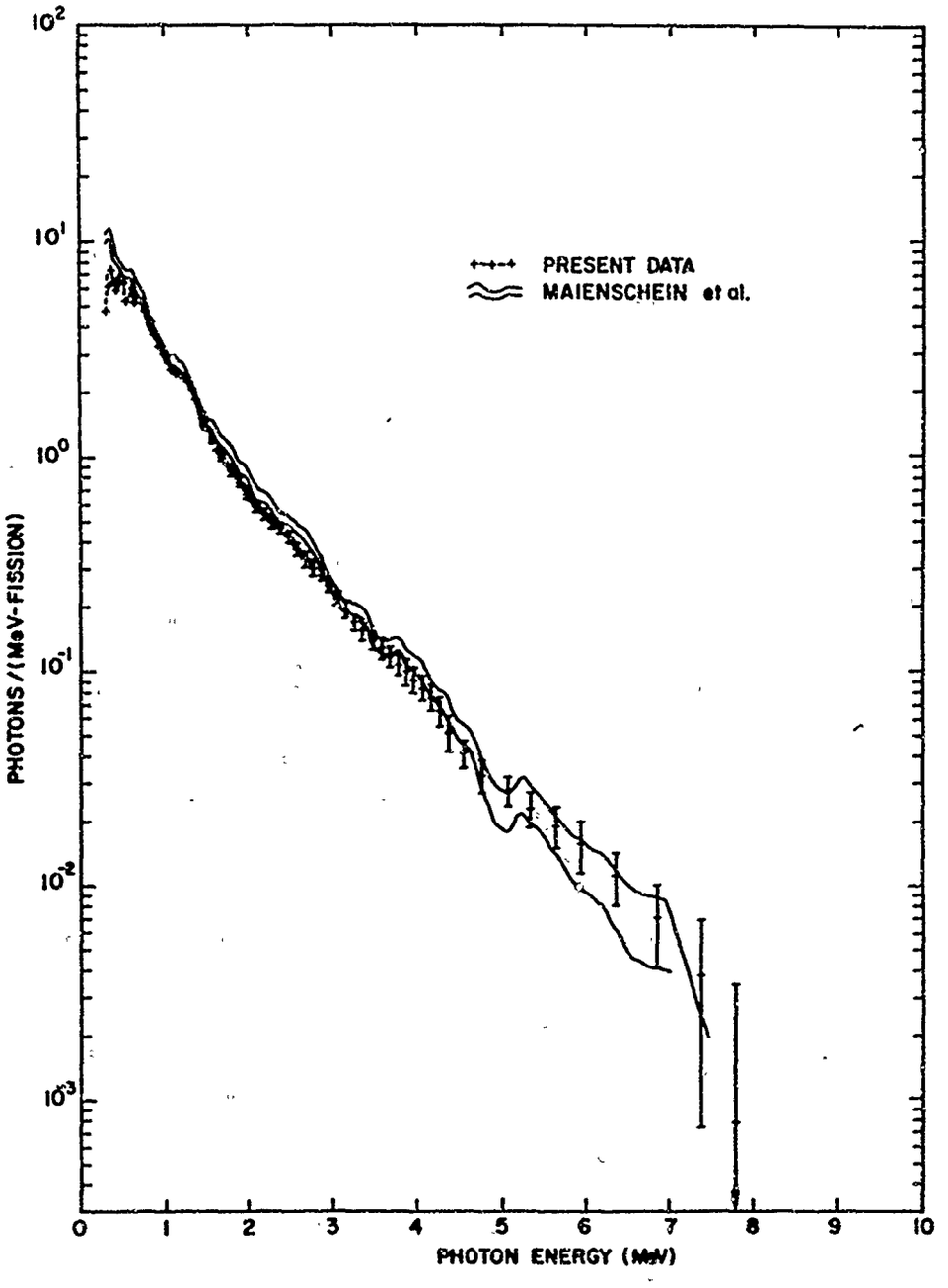

Figure 10. Prompt gamma-ray energy spectrum for the thermal-neutron fission of ^{235}U from the present measurement compared to the Oak Ridge National Laboratory results (Ref. 12). The structure indicated in the present data below 0.7 MeV may be seen better in the expanded energy scale in Fig. 6

Table 1

Energy emitted per fission in the form of prompt gamma rays and the number of gamma rays per fission for various gamma-ray energy intervals. The relative values for the total energy per fission above 0.14 MeV, $E\gamma$(TOT), for ^{235}U, ^{239}Pu and ^{252}Cf, are known to an accuracy of about 0.1 MeV/fission, while the overall error in absolute yield from 0.14 to 10 MeV, is estimated to be 0.3 MeV for $E\gamma$(TOT), including systematic errors.

Photon Energy Range (MeV)	Photons/Fission			MeV/Fission		
	^{235}U	^{239}Pu	^{252}Cf	^{235}U	^{239}Pu	^{252}Cf
0.14-0.3	0.83	1.27	1.27	0.181	0.275	0.282
0.3-0.5	1.32	1.47	1.86	0.53	0.60	0.76
0.5-0.7	1.18	1.22	1.61	0.71	0.74	0.96
0.7-1.0	1.19	1.10	1.07	1.02	0.94	0.91
1.0-1.5	1.07	1.00	0.84	1.34	1.24	1.04
1.5-2.0	0.461	0.450	0.442	0.80	0.79	0.78
2.0-2.5	0.258	0.268	0.292	0.582	0.606	0.66
2.5-3.0	0.158	0.175	0.183	0.434	0.482	0.503
3.0-4.0	0.143	0.173	0.160	0.490	0.597	0.550
4.0-5.0	0.050	0.071	0.058	0.220	0.318	0.254
5.0-6.0	0.021	0.027	0.019	0.116	0.145	0.102
6.0-7.0	0.0098	0.0104	0.0057	0.064	0.067	0.038
7.0-10.0	0.0027	0.0015	0.0004	0.019	0.019	0.0019
0.14-10.0	6.69	7.24	7.81	6.51	6.82	6.84

~ 0.1 MeV, as reported by Rau.[4] The average energy of the gamma quanta above 0.14 MeV, $\bar{E}_\gamma$, obtained directly from the ratio of the energy per fission to the number of photons per fission is 0.97, 0.94, and 0.88 for ^{235}U, ^{239}Pu, and ^{252}Cf, respectively.

6. DISCUSSION OF RESULTS

6.1 COMPARISON OF SPECTRA

The gross features of the spectral shapes for the three different cases of fission are similar. In particular, the absolute yields between 0.8 and 4.0 MeV are the same within about 20% for all three cases of fission (see Fig. 9). Below 0.7 MeV the ^{252}Cf data are roughly 50% higher than the ^{235}U data, and the ^{239}Pu results fall between the other two cases. Even though the error bars become large above 5.0 MeV, the data indicate that the ^{235}U and ^{239}Pu results are higher than those for ^{252}Cf. The reality of the above differences would be very questionable if each set of data had been obtained from a different laboratory.

The total prompt gamma-ray energy release per fission above 0.14 MeV, E_γ(TOT), given in Table 1, shows that the ^{252}Cf yield is equal to the ^{239}Pu yield, and both are only 5% larger than that for ^{235}U. Below 0.14 MeV, the yield drops off rapidly with decreasing energy until the x-ray region is reached. These values of E_γ(TOT), which varied between 6.51 and 6.84 MeV, are much larger than the value of 4.0 MeV predicted by Leachman and Kazek[1] for ^{252}Cf spontaneous fission and 4.9 MeV predicted by Terrell[2] for thermal-neutron fission of ^{235}U. Grover and Nagel[13] have shown that neutron-unstable nuclei with spins greater than 7/2 which can decay only to a spin 0 level decay preferentially by gamma-ray emission, even though the neutrons could decay with energies of several hundred keV. Taking the high-spin states of fission fragments into account, Thomas and Grover[14] obtained a value of 7.1 MeV for E_γ(TOT) for an average pair of fragments (^{96}Sr and ^{140}Xe). This value compares favorably with our experimental value of E_γ(TOT) = 6.51 ± 0.3 MeV

for $E_\gamma > 0.14$ MeV from ^{235}U. The total yield below 0.14 MeV is probably on the order of 0.1 MeV fission.

The similarity of the prompt gamma-ray energy per fission, $E_\gamma(TOT)$, for the three cases of fission is probably a result of the prompt neutron decay taking place before the gamma-ray decay. The neutrons take away as much energy as possible, and the energy that is left for gamma-ray decay, for the three cases of fission studied in the present measurements, is approximately independent of the A of the nucleus, the type of fission, or the initial spin of the nucleus. If there were a strong correlation with the initial spin, the nucleus with the higher initial spin would be expected to have the higher gamma-ray yield; however, our experimental results indicate a higher $E_\gamma(TOT)$ for ^{239}Pu than that for ^{235}U, whereas the initial spin of 1/2 for ^{239}Pu is lower than the spin of 7/2 for ^{235}U.

The difference in the shapes of the gamma-ray spectra, as reflected in the $\bar{E}_\gamma$ values of 0.97, 0.94, and 0.88 MeV/photon for ^{235}U, ^{239}Pu, and ^{252}Cf, respectively, may possibly be explained by the following arguments. The softer gamma-ray spectrum for ^{252}Cf is probably related to the higher level-density of the fission fragments for this case, or possibly to the nature of the levels, and the manner in which these parameters vary with the mass of the fission fragments. In a study of K x-ray yields as a function of fission fragment mass, Wehring and Wyman[15] found that for $^{235}U(n, F)$, the K x-ray yield was large only at the upper end of the light-fragment peak (at Z = 40-42) of the fission-fragment mass-yield curve. This is consistent with a higher level density at this high-mass end of the low-mass peak, and is a result of these nuclei being located within the edge of the region where deformed nuclei are found. The higher level density increases the probability of internal conversion, and thus increases the probability of K x-rays. These x-ray measurements, in fact, help define the boundary of the distorted-nucleus region. For ^{252}Cf, the light-mass peak completely straddles the region of distorted

nuclei, according to Fig. 12 of Reference 16, so that nearly all of the light-fragment yield falls in this region. This is consistent with the x-ray yields observed for ^{252}Cf by Glendenin, et al.[16] and Kapoor, et al.[17] At the high end of the mass yield curve, the same arguments hold. For ^{252}Cf, the upper end of the heavy-fragment mass-yield peak moves further into the distorted-nucleus region, further from the Z = 50, N = 82 stability lines. Similarly, for ^{239}Pu the lower peak of the mass-yield curve lies more in the distorted-nucleus region than that for ^{235}U, but less than that for ^{252}Cf, according to Fig. 12 of Reference 16. This is consistent with the order of the yields below 0.8 MeV.

In addition to the greater level density in the distorted-nucleus region, as mentioned above, the presence of rotational spectra in this region may provide a series of levels through which the excited nucleus may become preferentially deexcited through a large overall change in nuclear spin. Since the level spacing for rotational spectra is typically small, this type of deexcitation would be consistent with the observation of a smaller value of $\bar{E}_\gamma$ for ^{252}Cf.

6.2 VARIATION OF ϕ(E) WITH INCIDENT NEUTRON ENERGY

The comparison of the prompt gamma-ray yields presented in Fig. 9 shows nearly a factor of two greater yield for ^{252}Cf than for ^{235}U at about 0.2 MeV; at the high-energy end of the spectrum, there appears to be a significant disagreement, but of the opposite sign. In these measurements, the results in each case are effectively integrated over a large range of mass A of the fission fragments. The spectral yield from a narrow range of A, designated by ϕ_A(E), is expected to show appreciably larger differences in yields.

The variation of ϕ(E) for the three cases of fission studied in the present measurement indicates that the results depend on the mass-yield curve for the three different cases. If ϕ_A(E) is known as a function of A for thermal-neutron induced fission, it may be possible to combine this

information with the known data on mass-yield curves as a function of the energy E_n of the neutron inducing the fission and thus obtain an estimate for the variation of $\phi(E)$ with E_n. This possibility is attractive because of the great difficulty of measuring $\phi(E)$ at high E_n.

From this standpoint, it would be helpful to have data on the value of $\phi_A(E)$ versus A. With a relatively small modification of our equipment, work of this type could be carried out with the same spectrometer used for the present work. A "massless" fission foil and two fission-fragment detectors would be needed to measure the energy of both the heavy and the light fragment simultaneously. Of course, it would be difficult to separate the $\phi_A(E)$ for a particular narrow range of A in the light fragment region from those gamma rays emitted from the associated heavy fragment, since experimentally one measures the gamma rays from both fragments. However, this separation would not be needed when dealing with the same fissionable isotope in both the estimates of $\phi(E)$ at large E_n and the experiments at thermal-neutron energies. Of course, the statistics in some A regions would be very poor, so it would be helpful to use a number of fissioning isotopes to obtain additional information on the variation of the gamma-ray spectrum with A.

ACKNOWLEDGMENTS

Thanks are due to W. John of the Lawrence Radiation Laboratory for helpful discussions, to C. Young of LASL for the LSMUN code and patient discussions relating to its application, to F. K. Smith and J. G. Povelitis of LASL for the fabrication and loan of excellent, clean ^{239}Pu and ^{235}U foils, to L. Kull for early computations relating to angular distribution effects and energy loss in the fissionable material, to C. E. Creutz for his help as a summer participant, to Ed Beaver in early work with the LSMUN code, and to D. C. Imes for extensive help in LSMUN coding and plotting routines. Thanks are also due to J. R. Beyster for continued interest and helpful discussions.

REFERENCES

1. R. B. Leachman and C. S. Kazek, Jr., Phys. Rev. 104, 1511 (1957).

2. J. Terrell, Phys. Rev. 113, 527 (1959).

3. F. C. Maienschein, et al., Proc. U. N. Inter. Conf. Peaceful Uses of Energy, 2nd Geneva Conf., 1958, 15, 366 (1958).

4. F. E. W. Rau, Ann. Physik (7) 10, 252 (1963).

5. H. R. Bowman and S. G. Thompson, Proc. 2nd U. N. Inter. Conf. on Peaceful Uses of Atomic Energy, 15, Paper P/652, p. 212 (1958).

6. M. Hoffman, Phys. Rev. 135, B714 (1964).

7. M. V. Blinov, et al., Soviet Physics JETP 16, 1159 (1963).

8. L. Jarczyk, et al., Nucl. Inst. Meth. 17, 310 (1962).

9. Carl Young, LASL (Private Communication).

10. B. C. Cook, Nucl, Inst. Meth. 24, 256 (1963).

11. S. A. E. Johansson, Nucl. Phys. 60, 378 (1964).

12. R. W. Peelle, W. Zobel and F. C. Maienschein, "The Spectrum of Prompt Gamma Rays from Thermal Fission of ^{235}U", Submitted to ANS Meeting, Seattle, Washington, June, 1969 (Proc. ANS. Vol. 12, Part I)

13. J. R. Grover and R. J. Nagle, Phys. Rev. 134, B1248 (1964); J. R. Grover, Phys. Rev. 123, 267 (1962).

14. T. D. Thomas and J. R. Grover, Phys. Rev. 159, 980 (1967).

15. B. W. Wehring and M. E. Wyman, Phys. Rev. 157, 1083 (1967).

16. L. E. Glendenin and J. P. Unik, Phys. Rev. 140, B1301 (1965).

17. S. S. Kapoor, H. R. Bowman and S. G. Thompson, Phys. Rev. 140, 963 (1966).

UNCLASSIFIED
Security Classification

DOCUMENT CONTROL DATA - R & D

(Security classification of title, body of abstract and indexing annotation must be entered when the overall report is classified)

1. ORIGINATING ACTIVITY (Corporate author)	2a. REPORT SECURITY CLASSIFICATION
Gulf General Atomic Incorporated P. O. Box 608 San Diego, California 92112	Unclassified 2b. GROUP

3. REPORT TITLE

Measurement of Prompt Gamma-Rays from Thermal-Neutron Fission of ^{235}U and ^{239}Pu, and From Spontaneous Fission of ^{252}Cf

4. DESCRIPTIVE NOTES (Type of report and inclusive dates)

Annual Summary Report - May 15, 1967 through November 30, 1968

5. AUTHOR(S) (First name, middle initial, last name)

V. V. Verbinski and R. E. Sund

6. REPORT DATE	7a. TOTAL NO. OF PAGES	7b. NO. OF REFS
April 5, 1969	45	17

8a. CONTRACT OR GRANT NO.	9a. ORIGINATOR'S REPORT NUMBER(S)
DASA 01-67-C-0088 b. PROJECT NO. PA 010 c. d.	GA-9148 9b. OTHER REPORT NO(S) (Any other numbers that may be assigned this report) DASA-2234

10. DISTRIBUTION STATEMENT

Each transmittal of this document outside the agencies of the U. S. Government must have prior approval of Director, Defense Atomic Support Agency, Washington, D. C. 20305

11. SUPPLEMENTARY NOTES	12. SPONSORING MILITARY ACTIVITY
	Director Defense Atomic Support Agency Washington, D. C. 20305

13. ABSTRACT

The prompt gamma-ray spectra were measured for the thermal-neutron fission of ^{235}U, and ^{239}Pu and for the spontaneous fission of ^{252}Cf. All three measurements utilized the same detector and the same source detector geometry so that the results should indicate accurately the differences in the gamma-ray spectra and yields for the three isotopes. The yield of low-energy gamma-rays, E_γ, was the lowest for ^{235}U, and the total gamma-ray energy per fission event was smallest for this case. The yield below about 0.5 MeV was about twice as great for ^{252}Cf, which had the softest gamma-ray spectrum and the largest E_γ. The spectral shape is probably related to the fact that the heavier fissionable isotopes produce fission fragments whose mass-distribution peaks fall farther into the distorted-nucleus region, away from the N = 50 subshell for the light fragments and from the N = 82 subshell for the heavier fragments.

DD FORM 1 NOV 65 1473

UNCLASSIFIED
Security Classification

14. KEY WORDS	LINK A		LINK B		LINK C	
	ROLE	WT	ROLE	WT	ROLE	WT
Prompt gamma rays						